Laser intracavity absorption

Helen K. Holt
National Bureau of Standards, Washington, D.C. 20234
(Received 3 October 1974)

The characteristics of a laser with an intracavity absorption cell have been calculated for the case in which the gain atoms are homogeneously broadened and the absorber atoms are inhomogeneously broadened. The sensitivity of the laser intensity to the density of absorbers is determined.

I. INTRODUCTION

Recently, there has been interest in using laser intracavity absorption to detect small quantities of atoms or molecules.[1,2] Typically such experiments consist of a laser cavity containing a gain cell (a dye cell) and an absorption cell filled with the sample gas. The laser frequency is tuned through one or more resonance frequencies of the sample atoms, and the laser output intensity decreases over the absorption line in a way which depends upon the density of the sample atoms. Because the laser intensity is much more dependent on intracavity losses than on extracavity ones, this method promises increased sensitivity over standard techniques.

The purpose of the present paper is to treat the above experiment for the single-mode case, in which the gain atoms are assumed to be homogeneously broadened and the absorbers inhomogeneously broadened. The paper begins by describing a single-mode dye laser with no absorber and continues to describe the properties of the absorber and then to obtain the output with both gain atoms and absorbers present. The method is semiclassical.[3]

II. LASER WITHOUT ABSORPTION CELL

We start with the problem of the gain atom. Assume it has two levels, a (upper) and b (lower), with widths γ_a and γ_b, respectively. Atoms are excited to state i at a rate λ_i (number/cm^3 sec). The laser light is characterized by an electric field in the x direction of magnitude $E\cos(\nu t+\varphi)\times\sin Kz$, where z is measured along the laser axis. If a and b are the amplitudes of the states, and $\rho_{aa}=aa^*$, $\rho_{bb}=bb^*$, and $\rho_{ab}=ab^*$, then the time-dependent Schrödinger equation gives[4]

$$\dot{\rho}_{aa}=\lambda_a-\gamma_a\rho_{aa}-\mathrm{Re}[(ip_1^*/\hbar)E\sin(Kz)e^{i(\nu t+\varphi)}\rho_{ab}], \tag{1}$$

$$\dot{\rho}_{bb}=\lambda_b-\gamma_b\rho_{bb}+\mathrm{Re}[(ip_1^*/\hbar)E\sin(Kz)e^{i(\nu t+\varphi)}\rho_{ab}], \tag{2}$$

$$\dot{\rho}_{ab}=-(\gamma_{ab}+i\omega_{ab})\rho_{ab}-(ip_1E/2\hbar)e^{-i(\nu t+\varphi)}\sin(Kz)(\rho_{aa}-\rho_{bb}), \tag{3}$$

where $\gamma_{ab}=\frac{1}{2}(\gamma_a+\gamma_b)$ and $p_1\equiv e\int\varphi_a^*x\varphi_b\,d\tau$.

The solution to these equations is found by a Fourier-series method.[4] It is

$$\rho_{ab}=\frac{p_1E}{4\hbar}e^{-i(\nu t+\varphi)}\frac{2N_{ab}}{(\nu-\omega_{ab}+i\gamma_{ab})}\sum_{n=0}^{\infty}B_n\sin(2n+1)Kz, \tag{4}$$

where $N_{ab}=\lambda_a/\gamma_a-\lambda_b/\gamma_b$ is the unperturbed inversion density, and the B_n's are determined by recursion relations.[4] Here

$$B_0=\frac{2}{1+8\alpha_1G_1+(1+8\alpha_1G_1)^{1/2}}, \tag{5}$$

where

$$\alpha_1\equiv\frac{|p_1|^2E^2}{8\hbar^2\gamma_a\gamma_b},\quad G_1=\frac{\gamma_{ab}^2}{(\nu-\omega_{ab})^2+\gamma_{ab}^2}.$$

The induced dipole moment per unit volume is

$$P(z,t)=2\,\mathrm{Re}(\rho_{ab}p_1^*). \tag{6}$$

To compute the output, one needs

$$P(t)=(2/L)\int_0^L P(z,t)\sin(Kz)\,dz$$

$$=\mathrm{Re}[(C+iS)e^{-i(\nu t+\varphi)}], \tag{7}$$

where L is the cavity length. The output is obtained from the following equation,[3] balancing gain and loss:

$$-S/E=\epsilon_0/Q, \tag{8}$$

where Q is the cavity "Q". Equations (4), (6), and (7) give

$$S=\frac{-|p_1|^2E}{\hbar}\frac{N_{ab}}{\gamma_{ab}}\frac{l_1}{L}G_1B_0, \tag{9}$$

where l_1 is the length of the gain cell. Equations (8) and (9) give

$$G_1B_0=\frac{(N_{ab})_{\mathrm{th}}}{N_{ab}}\equiv n_1^{-1}, \tag{10}$$

where $(N_{ab})_{\mathrm{th}}$ is that value of N_{ab} for which $\alpha_1=0$

at $\nu = \omega_{ab}$. The solution of Eq. (10) for α_1 is

$$8\alpha_1 G_1 = \tfrac{1}{2}(4u - 1 - \sqrt{8u+1}), \tag{11}$$

where $u \equiv G_1 n_1$. For some purposes, it is useful to approximate Eq. (11) by

$$6\alpha_1 G_1 \cong u - 1 \quad (u \geq 1)$$
$$= 0 \quad (u \leq 1). \tag{12}$$

This is accurate to better than 10% for u smaller than 3, and very good near threshold. From Eq. (12) the maximum value of α_1, for $\nu = \omega_{ab}$, is $(\alpha_1)_{\max} = \frac{1}{6}(n_1 - 1)$. α_1 goes to zero at $u = 1$ or $(\nu - \omega_{ab})/\gamma_{ab} = \pm(n_1 - 1)^{1/2}$. The full width at half-maximum is $[2(n_1 - 1)]^{1/2}$. Curves of $6\alpha_1$ as a function of tuning are shown in Fig. 1. The solid curves are derived from Eq. (11), the dashed ones from Eq. (12).

III. LASER WITH INTERNAL ABSORPTION CELL

Now consider the inhomogeneously broadened absorber atoms. Assume they have two levels, c (upper) and d(lower), with widths γ_c and γ_d, respectively. The equations for the density matrix components are the same here as Eqs. (1)–(3) except for the fact that they now apply in the rest frame of the moving atom, so that z is now time dependent. The solution for S in this case is[4]

$$S = \frac{-|p_2|^2 E N_{cd}}{2\hbar\gamma_{cd}} \frac{l_2}{L} \int_{-\infty}^{\infty} \mathrm{Re}(B_0 R_0) W(v_z)\, dv_z, \tag{13}$$

where

$$R_0 = i\gamma_{cd}\left(\frac{1}{\nu - \omega_{cd} - Kv_z + i\gamma_{cd}} - \frac{1}{\nu - \omega_{cd} + Kv_z - i\gamma_{cd}}\right)$$

and

$$W(v_z)\, dv_z = \frac{1}{\sqrt{\pi}} e^{-(v_z/u)^2} \frac{dv_z}{u},$$

the Maxwellian velocity distribution. Here B_0 is found from the recursion relations,[4] but, unlike the zero-velocity case, there is no simple exact expression for B_0. For very low intensities or saturation parameters (α), one may use $B_0 \cong 1 - 2\alpha\,\mathrm{Re}R_0$. This is equivalent to the "third-order" result of Lamb[3] and is good up to $\alpha \cong 0.05$. Another approximation is

$$B_0 \cong \frac{1}{1 + 2\alpha\,\mathrm{Re}R_0}. \tag{14}$$

This is good to $\lesssim 10\%$ up to $\alpha \sim 1$ and will be used here for now in order to get an analytic solution.

In the Doppler limit ($\gamma_{cd}/Ku \ll 1$), $\mathrm{Re}(B_0 R_0)$, where B_0 is given by Eq. (14), can be integrated over the velocity distribution to yield

$$S = \frac{-|p_2|^2 E N_{cd} (\pi)^{1/2}}{\hbar K u} \frac{l_2}{L} e^{-(\nu - \omega_{cd}/Ku)^2} \times \frac{1}{(1 + 2\alpha_2)^{1/2}} \left(\frac{1 + \alpha_2 G_2}{1 + 2\alpha_2 G_2}\right), \tag{15}$$

where the quantities here are the same as those previously defined for the gain atoms with 1, a, and b replaced by 2, c, and d. Equation (15) is correct only for

$$\alpha_2^2 \ll \left(\frac{\nu - \omega_{cd}}{\gamma_{cd}}\right)^2 (1 + 2\alpha_2).$$

For the case $\nu = \omega_{cd}$, the quantity $[1/(1+2\alpha_2)^{1/2}] \times [(1 + \alpha_2 G_2)/(1 + 2\alpha_2 G_2)]$ is replaced by $[1/(1+4\alpha_2)^{1/2}]$.

In order to calculate the output of a laser with both a gain cell and an absorber, we add Eqs. (9) and (15) to obtain $S_T = S_1 + S_2$. Then, from the equation $S_T/E = -\epsilon_0/Q$ results

$$\frac{2n_1 G_1}{1 + 8\alpha_1 G_1 + (1 + 8\alpha_1 G_1)^{1/2}} - \frac{\bar{k}}{(1 + 2\lambda\alpha_1)^{1/2}} \left(\frac{1 + \lambda\alpha_1 G_2}{1 + 2\lambda\alpha_1 G_2}\right) = 1. \tag{16}$$

Here $\lambda = \alpha_2/\alpha_1$; λ determines how much the absorbers are saturated for a given gain saturation parameter. Also $\bar{k} = ke^{-y^2}$, where

$$y = \left(\frac{\nu - \omega_{cd}}{Ku}\right),$$

$$k = \frac{|p_2|^2}{|p_1|^2} \frac{(\pi)^{1/2}\gamma_{ab}}{Ku} \frac{l_2}{l_1} \frac{|N_{cd}|}{(N_{ab})_{\mathrm{th}}}.$$

In Eq. (16), $(N_{ab})_{\mathrm{th}}$ is the previously defined threshold value of N_{ab} for the case $\bar{k} = 0$. If σ = (absorption coefficient) × (absorption length), then

$$\bar{k} = \frac{\sigma_2}{(\sigma_1)_{\mathrm{th}}}$$

and

$$n_1 = \frac{\sigma_1}{(\sigma_1)_{\mathrm{th}}}.$$

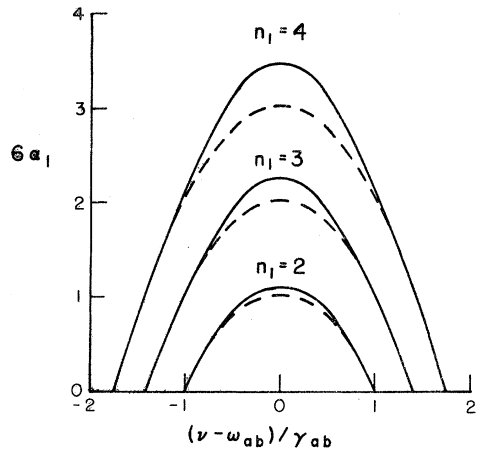

FIG. 1. $6\alpha_1$, proportional to the power output of a single-mode homogeneously broadened laser, as a function of cavity tuning. Solid curve, from Eq. (11); dashed curve, from Eq. (12).

$(\sigma_1)_{th}$ is defined analogously to $(N_{ab})_{th}$; it is the threshold gain.

Equation (16) can be used to express α_1 as a function of n_1, k, y, and λ. The simplest case is that for which $\lambda \to 0$ (no absorber saturation). Then α_1 is given by Eq. (11) or Eq. (12) with

$$u = n_1 G/(1+\bar{k}) .$$

For the experiments in question, the effective homogeneous width of the dye is large compared to the Doppler width of the absorber so that, in the region of the absorption, G_1 can be replaced by 1. Then Eq. (12) gives

$$6\alpha_1 \cong [n_1/(1+\bar{k})] - 1 . \tag{17}$$

Figure 2 shows $6\alpha_1$ as a function of y for $n_1 = 2$ and for several values of k. Only half of each curve has been shown since they are symmetrical about $y = 0$.

If λ is different from zero, there is a central resonance of width near $2\gamma_{cd}$, which will be discussed later. The effect of absorber saturation on the rest of the absorption curve will be considered now. For the case $n_1 \lesssim 2$ and $\lambda \leq 6$, one can expand the square roots in Eq. (16) to obtain

$$\frac{n_1}{1+6\alpha_1} - \frac{\bar{k}}{1+\lambda\alpha_1}\left(\frac{1+\lambda\alpha_1 G_2}{1+2\lambda\alpha_1 G_2}\right) = 1 . \tag{18}$$

Since we have assumed $\gamma_{cd} \ll Ku$ (Doppler limit), we can consider the region away from the central narrow resonance by taking the limit $(\nu - \omega_{cd})/\gamma_{cd} \to \infty$ or $G_2 \to 0$. With these approximations, Eq. (18) gives α_1 as the solution to a quadratic equation which is readily solved for each individual case. In particular, for $\lambda = 6$, $\alpha_1 = \frac{1}{6}(n_1 - 1 - \bar{k})$, as shown in Fig. 3. This expression is larger than the $\lambda = 0$ solution by a factor $1+\bar{k}$. Therefore, if $\alpha_1 = 0$ for some y, increasing λ from 0 to 6 only influences the midpoints of the curve of α_1 vs y, not the end points.

If λ is greater than about 6, one can find α_1 as a function of $\bar{k}$ graphically by plotting

$$\frac{\bar{k}}{(1+2\lambda\alpha_1)^{1/2}} \quad \text{and} \quad \frac{n_1}{(1+6\alpha_1)} - 1$$

as functions of α_1 and finding their intersection for various values of $\bar{k}$. The results of such a determination, for $n_1 = 2$, are shown in Fig. 4(a). It can be shown that if λ is ≤ 12, α_1 is zero for $\bar{k} = n_1 - 1 = 1$; for $\lambda > 12$ (and $n_1 = 2$), the value of $\bar{k}$ needed to make α_1 zero is $[(\lambda+12)/(48\lambda)^{1/2}] > 1$. Thus, for $\lambda > 12$, saturation of the absorber affects the end point as well as the midpoints of the curve of α_1 vs y. This effect is shown in Fig. 4(b), where intensity-vs-tuning curves are plotted for $\lambda = 60$ and $\lambda = 0$. The $\lambda = 60$ curves are derived from Fig. 4(a).

In order to calculate the shape of the narrow central resonance, we use Eq. (18) with $G_2 \neq 0$. [For more accurate results, one could solve Eq. (16) numerically, with the appropriate correction at line center.] Because we assumed the Doppler limit, y is taken to be zero over the widths of the resonances. Figure 5 shows the shapes of the resonances for $n_1 = 2$, for several values of k, and for the cases $\lambda = 6$ and $\lambda = 3$. One can see that in the middle range of k, where the peaks are largest, the heights of the $\lambda = 3$ peaks are about half the heights of the $\lambda = 6$ peaks. It can be shown, using Eq. (18), that $6[\alpha_1(0) - \alpha_I(\infty)] \cong 0.025\lambda$ at $k = 0.5$. The heights of the resonances increase over the range $k = 0$ to about $k = 0.8$ and then decrease to zero at $k = 1$. The widths are approximately given by $2[1+\lambda\alpha_1(\infty)]$ over the range $k = 0.2$–0.8 and fall below that as k approaches 1.

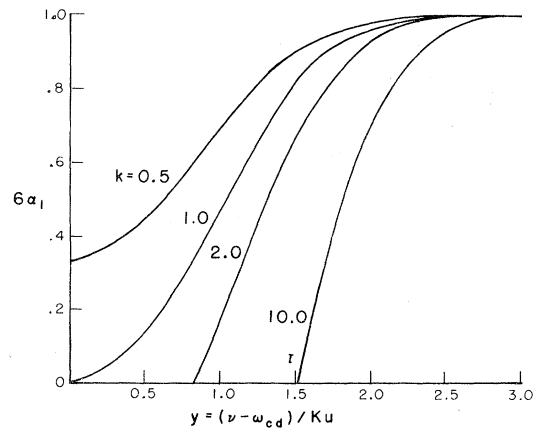

FIG. 2. $6\alpha_1$ as a function of cavity tuning with an absorber present for $\lambda = 0$ and $n_1 = 2$.

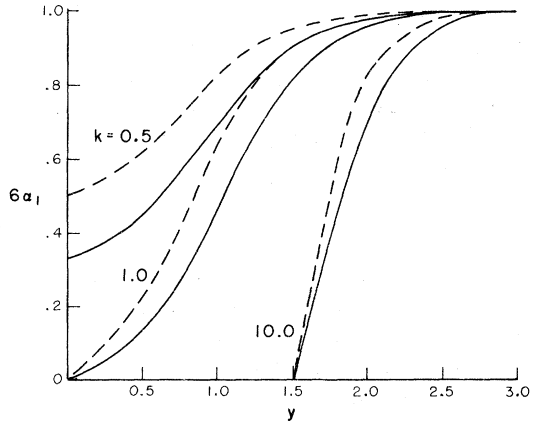

FIG. 3. Effect of absorber saturation on the intensity-vs-tuning curves. Dashed curves, $\lambda = 6$; solid curves, $\lambda = 0$. $n_1 = 2$ for all.

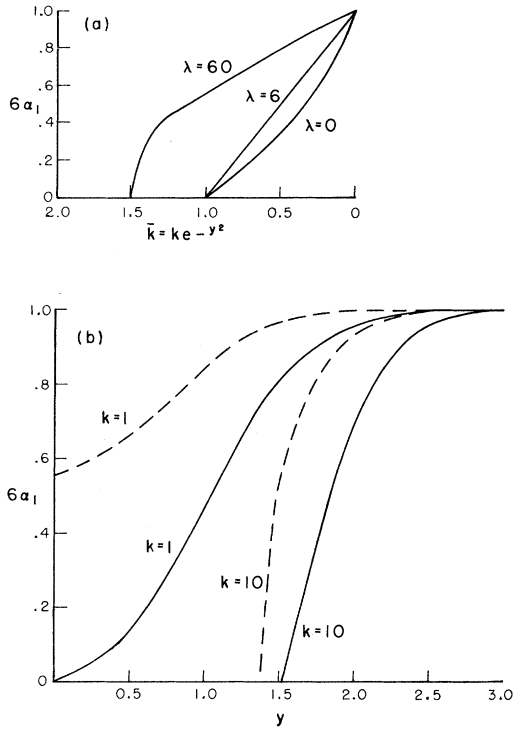

FIG. 4. (a) $6\alpha_1$ as a function of $\bar{k}$ for $\lambda=0$, 6, and 60, and $n_1=2$. (b) $6\alpha_1$ vs y for $n_1=2$, $k=1$ and 10. Solid curves, $\lambda=0$; dashed curves, $\lambda=60$.

IV. DETECTION WITH EXTERNAL CELL

The calculation so far has completed the derivation of the power output vs tuning of a single-mode laser consisting of homogeneously broadened gain atoms and inhomogeneously broadened absorption

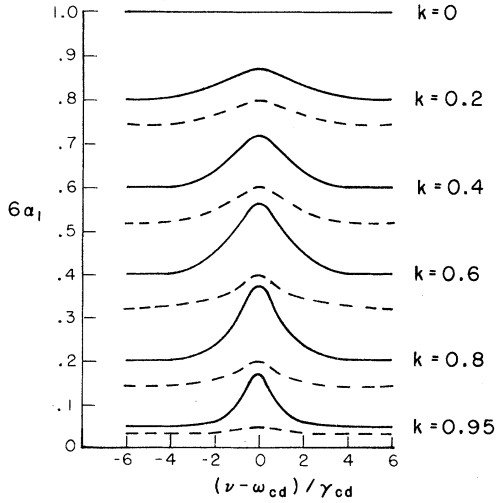

FIG. 5. Narrow central resonances for $n_1=2$ and several values of k. Solid curves, $\lambda=6$; dashed curves, $\lambda=3$.

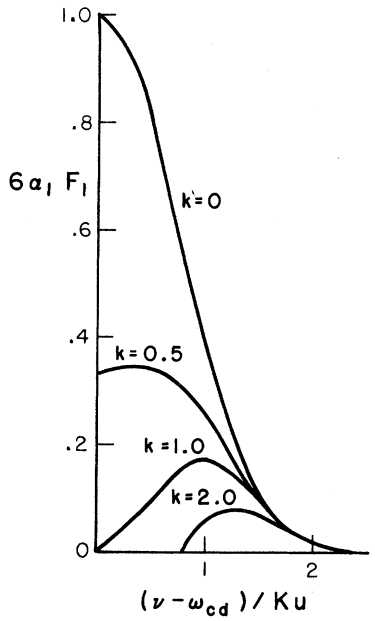

FIG. 6. $6\alpha_1 F_1$ vs y, where $F_1=e^{-y^2}$, for the case $n_1=2$, $\lambda=0$.

atoms. In order to detect small quantities of absorber atoms, one can tune the laser over the absorption curve and measure the decrease in power output as a function of tuning. One very sensitive way of measuring this decrease is to use an external cell filled with the same atoms as the internal absorption cell and measure the fluorescence from the external cell. The detected intensity is obtained by multiplying $\alpha_1(y)$, where $y=(\nu-\omega_{cd})/Ku$, by the external absorber detection efficiency, a function of y. If the region of the external cell viewed by the fluorescence detector is l_3, and the absorption length leading up to that region is l_3',

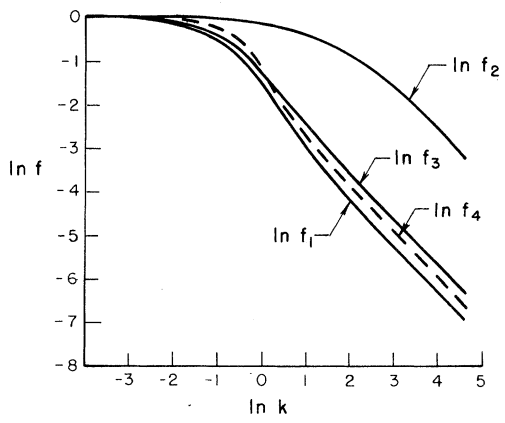

FIG. 7. $\ln f_i$ vs $\ln k$, where f_i is proportional to the integrated detector signal.

then the detection efficiency is proportional to

$$(e^{(-l_3'/l_3)\sigma e^{-y^2}})(1-e^{-\sigma e^{-y^2}}) \equiv F,$$

where σ is the absorption coefficient times l_3. For $l_3'=0$ and $\sigma \ll 1$, $F \cong \sigma \epsilon^{-y^2}$. Figure 6 shows $6\alpha_1 e^{-y^2}$, where α_1 is calculated for $n_1=2$, $\lambda=0$. This is proportional to the intensity which would be measured by the fluorescence detector if a single-mode laser were scanned in frequency. The integrated fluorescence intensity is also a sensitive measure of the absorber density. Figure 7 shows $\ln f_i$ vs $\ln k$, where f_i is the integrated detector signal:

$$f_i = \frac{\int_{-\infty}^{\infty} 6\alpha_1(y) F_i(y)\, dy}{\int_{-\infty}^{\infty} F_i(y)\, dy}.$$

Here

$$F_1 = e^{-y^2},$$
$$F_2 = e^{-10e^{-y^2}}(1-e^{-10e^{-y^2}}),$$
$$F_3 = e^{-e^{-y^2}}(1-e^{-(0.1)e^{-y^2}}).$$

For $i=1 \rightarrow 3$, α_1 was calculated for $n_1=2$, $\lambda=0$. A fourth case, f_4, was calculated using F_1 and the case $n_1=2$, $\lambda=6$, for α_1. The integrations were performed numerically.

In case 1, f_1 is reduced to $1/e$ for $\ln k=-0.4$ or $k=0.67$. Since $k=(\sigma_2)/(\sigma_1)_{\text{th}}$, this is for $\sigma_2=(0.67)\times(\sigma_1)_{\text{th}}$. If $(\sigma_1)_{\text{th}}$ is determined by the mirror reflectivity, it can be typically of the order of 0.01, so that the signal is reduced to $1/e$ for $\sigma_2 \cong 0.0067$. This can be compared with the sensitivity of a conventional absorption experiment in which $I=I_0 e^{-\sigma_2}$, so that the signal falls by $1/e$ at $\sigma_2=1$. The improvement in the present case is thus of the order of a factor of 150. Even greater enhancement is achieved in the multimode case.[1,2]

---

[1]R. A. Keller, J. D. Simmons, and D. A. Jennings, J. Opt. Soc. Am. 63, 1552 (1973), and references therein.
[2]T. W. Hänsch, A. L. Schawlow, and P. E. Toschek, IEEE J. Quantum Electron. QE-8, 802 (1972).
[3]W. E. Lamb, Jr., Phys. Rev. 134, A1429 (1964).
[4]H. K. Holt, Phys. Rev. A 2, 233 (1970).